

# Aggressive or Imperceptible, or Both: Network Pruning Assisted Hybrid Byzantines in Federated Learning

Emre Özfatura<sup>†</sup>, Kerem Özfatura\*, Alptekin Küpçü\*, Deniz Gündüz<sup>†</sup>

\*KUIS AI LAB

Koç University

<sup>†</sup>IPC LAB

Imperial College London

**Abstract**—Federated learning (FL) has been introduced to enable a large number of clients, possibly mobile devices, to collaborate on generating a generalized machine learning model thanks to utilizing a larger number of local samples without sharing to offer certain privacy to collaborating clients. However, due to the participation of a large number of clients, it is often difficult to profile and verify each client, which leads to a security threat that malicious participants may hamper the accuracy of the trained model by conveying poisoned models during the training. Hence, the aggregation framework at the parameter server also needs to minimize the detrimental effects of these malicious clients. A plethora of attack and defence strategies have been analyzed in the literature. However, often the Byzantine problem is analyzed solely from the outlier detection perspective, being oblivious to the topology of neural networks (NNs).

In the scope of this work, we argue that by extracting certain side information specific to the NN topology, one can design stronger attacks. Hence, inspired by the sparse neural networks, we introduce a hybrid sparse Byzantine attack that is composed of two parts: one exhibiting a sparse nature and attacking only certain NN locations with higher sensitivity, and the other being more silent but accumulating over time, where each ideally targets a different type of defence mechanism, and together they form a strong but imperceptible attack. Finally, we show through extensive simulations that the proposed hybrid Byzantine attack is effective against 8 different defence methods. Our code is available at <https://github.com/CRYPTO-KU/FL-Byzantine-Library>

## I. INTRODUCTION

Federated learning (FL) [31] become de-facto *collaborative learning* framework where a large number of clients optimize their model, e.g., neural network (NN) weights, locally by utilizing their personal data and then seek consensus on the global model through the exchange of local models, where this process is often performed through multiple consecutive iterations. While local optimization helps keep the personal data private, the consensus phase helps reduce the generalization error. In this work, we focus on *centralized* and *synchronous* FL setup [26], [31], where a central parameter server (PS) orchestrates the consensus phase by executing an aggregation policy for the local models received from all the participating clients and following the aggregation, the new

model is conveyed to the clients for the next round of local optimization/training.

In practice, FL is designed to facilitate collaborative learning over a large number of clients, where it is often challenging to profile and verify clients, especially when the variance among the updates from the clients' is very high [19] or when the identification metric is solely based on geometric distance [38]. To be more specific, this can be due to non-identically distributed client data or because some of the clients may act maliciously and aim to sabotage the learning process either individually or by colluding with other malicious clients. In the literature, this type of attempt is referred to as a poisoning attack [1], [4], [17], [41], where the malicious clients send a poisoned model to the PS in compliance with a predefined attack mechanism. These attacks can be *targeted* [1], [4], [47] or *untargeted* [6], [48], based on whether the objective is the model to fail only certain tasks, e.g., miss-classification of certain classes, or fail to perform any task [2], [4], [17], [41]. Besides, the attack is not always visible during the training; the model performs well for the training data but lacks generalization at test time, particularly performing poorly on samples with a certain triggering pattern, often referred to as a backdoor attack [1].

In the scope of this work, we limit our focus to untargeted model poisoning attacks, often known as Byzantine attacks, in FL. The design of the Byzantine attacks, under various assumptions, e.g., the training data that adversaries can access or the information they can infer, has been extensively studied in the literature [2], [14], [39], [50]. To overcome the detrimental impact of malicious clients, the design of a robust aggregator that neutralizes the poisoned models from different aspects has also been studied in the literature [6], [36], [52]. Many of the defence methods consider poisoned models as outliers and suggest eliminating statistically suspicious ones before using conventional aggregation functions like averaging [6], [12], [33], or some [8], [52] of them directly redesign the aggregation function to generate a good representation model for the benign clients, e.g., geometric mean, and finally some of them, rather than eliminating suspicious models, sanitize all the models before the executing the aggregation function

[10], [21], [24], [37]. Apart from these methods, some works in the literature suggest more complicated frameworks, where the defence strategy either utilizes extra data at the PS such as [7], [49] or profiles the clients over time and assigns a trust score to each of them [4], [33]. Recent work also explores a game-theoretic approach to dynamically selecting a different robust aggregator in each update between PS and clients. [50].

From the design perspective, an effective attack should be strong and imperceptible [2], [14], [39]. Hence, attacks often take advantage of the curse of dimensionality (that is, NNs have a large number of weights) and the variation among the benign models due to the data distribution among the clients since, in practice, the data is distributed in a non-iid manner. As the variation among the benign models increases, the feasible space for the Byzantines, where they do not look like outliers, also expands. Thus, as a counter strategy, some of the recent works utilize variance reduction techniques designed for distributed learning in order to shrink the feasible space of Byzantine attacks [18], [24], [25], [34], [35], [45], [53]. One of the popular approaches is to employ momentum SGD as a local optimizer and perform aggregation over the momentum terms; it has been shown that the use of local momentum enhances the robustness against the Byzantine attacks [11], [15], [24], [54].

Although there are various successful Byzantine attack designs, there is still a lack of a universal attack design that is effective against different types of defence mechanisms simultaneously. To be more precise, as we discuss in more detail later, while some Byzantine designs are more effective against defences that investigate index-wise outlier values, some are more effective against defence mechanisms that utilize geometric distance as a metric to detect anomalies. Therefore, in the scope of this work, we seek an answer to whether it is possible to **design a universally effective yet computationally low-cost Byzantine attack strategy**. Another important aspect often ignored in the design of Byzantine attacks is the structure of the NN. To be more precise, **certain weights might be more vulnerable against perturbations, and this prior knowledge can be utilized to enhance attack**. To the best of our knowledge, this is the first work that utilizes the inherited information from the neural network topology to modify Byzantine attacks. The contributions of this work can be summarized as follows

- We introduce a novel Byzantine attack framework consisting of two parts, each designed to avoid either index-wise elimination or geometric distance based investigation; hence, their combination is effective against both types of defences and does not require prior knowledge regarding the defence mechanism.
- Contrary to the existing Byzantine designs, we utilize side information extracted from the network architecture through a network pruning framework, which locates the possible sensitive weights and enhances this side information to generate stronger yet imperceptible attacks.
- Finally, through extensive simulations over different NN networks, datasets, and defence mechanisms, we show the

TABLE I: Notations

Notation	Description
$\mathcal{K}_b, \mathcal{K}_m$ and $\mathcal{K} = \mathcal{K}_b \cup \mathcal{K}_m$	Set of benign, malicious, and all clients, respectively
$k_b, k_m$ and $k$	Number of benign, malicious, and all clients, respectively
$\theta_{i,t}, \mathbf{g}_{i,t}$ , and $\mathbf{m}_{i,t}$	Model, gradient, and momentum vector of client $i$ at iteration $t$ , respectively.
$\bar{\mathbf{m}}_t, \hat{\mathbf{m}}_t, \tilde{\mathbf{m}}_t$	Reference, aggregated, and benign consensus momentum at iteration $t$ , respectively
$\delta, \mathbf{e}$	Sparsity ratio and the corresponding mask vector, respectively

effectiveness of our approach by reducing test accuracy up to 60% in IID simulations and diverging the model training completely in the non-IID simulations.

#### A. Federated Learning (FL) with Byzantines

**Notation:** We use **bold** to denote vectors, i.e.,  $\mathbf{v}$  and capital calligraphic letters, e.g.,  $\mathcal{V}$ , to denote sets. When we have an ordered set of vectors  $\mathcal{V} = \{\mathbf{v}_1, \dots, \mathbf{v}_i, \dots, \mathbf{v}_k\}$ , we use subscript index to identify  $i^{th}$  vector in the set,  $i \in [k]$ , and use double subscript  $\mathbf{v}_{i,t}$ , particularly when it is changing over time/iteration. For slicing operation, we use  $[\cdot]$ , such as  $\mathbf{v}[j]$  for selecting  $j^{th}$  index of a vector. We use  $\|\cdot\|_p$  to denote the  $p$ -norm of a vector and we use  $\|\cdot\|$  without  $p$  we refer  $l_2$  norm. We use  $\langle \cdot, \cdot \rangle$  for the inner product between two vectors. In Table I, we list the widely used variables in this paper.

The objective of FL is to solve the following parameterized optimization problem over  $k$  clients in a distributed manner

$$\min_{\theta \in \mathbb{R}^d} f(\theta) = \frac{1}{k} \sum_{i=1}^k \underbrace{\mathbb{E}_{\zeta_{i,t} \sim \mathcal{D}_i} f(\theta, \zeta_i)}_{:= f_i(\theta)}, \quad (1)$$

where  $\theta \in \mathbb{R}^d$  denotes the model parameters, e.g., weights of a neural network,  $\zeta_{i,t}$  is the randomly sampled mini-batch,  $\mathcal{D}_i$  denotes the dataset of client  $i$ , and  $f$  is the problem-specific empirical loss function. At each iteration of FL, each client aims to minimize its local loss function  $f_i(\theta)$  using *SGD*. Then, the clients seek a consensus on the model with the help of the PS.

In this work, following the previous works [24], [54], we focus on a particular FL framework where the consensus step is performed by aggregating the local momentum of the clients at the end of each optimization step  $t$ , which is later used by PS to update the global model.

---

#### Algorithm 1 FL with Robust Aggregator and Byzantines

---

- 1: **Input:**  $\eta, AGG(\cdot), Attack(\cdot)$
  - 2: **Output:** Consensus model:  $\theta_T$
  - 3: **for**  $t = 1, \dots, T$  **do**
  - 4:     **Client side:**
  - 5:     **for**  $i = 1, \dots, k$  **do** in parallel
  - 6:         Receive:  $\theta_{t-1}$  from PS
  - 7:         **if**  $i \in \mathcal{K}_b$  **then**
  - 8:             Update local model:  $\theta_{i,t} \leftarrow \theta_{t-1}$
  - 9:             Compute SGD:  $\mathbf{g}_{i,t} \leftarrow \nabla_{\theta} f_i(\theta_{i,t}, \zeta_{i,t})$
  - 10:             Update Momentum:  $\mathbf{m}_{i,t} = (1 - \beta)\mathbf{g}_{i,t} + \beta\mathbf{m}_{i,t-1}$
  - 11:         **else**
  - 12:              $\mathbf{m}_{i,t} \leftarrow Attack(\mathcal{H}_t)$
  - 13:     **Server side:**
  - 14:     Aggregate local updates:  $\bar{\mathbf{m}}_t \leftarrow AGG(\mathbf{m}_{1,t}, \dots, \mathbf{m}_{k,t})$
  - 15:     Update the server model:  $\theta_t \leftarrow \theta_{t-1} - \eta_t \bar{\mathbf{m}}_t$
-

TABLE II: Comparison of the defence methods

Defence mechanism	Identification Metric	Defence
Centered Clipping [24]	Euclidean distance	Sanitization with clipping
Krum & Multi-Krum [6]	Euclidean distance	Elimination
Bulyan [12]	Euclidean distance	Elimination
Trimmed mean [52]	Index-wise statistics	Elimination
Centered median [52]	Index-wise statistics	Index-wise Median
SignSGD [3], [23]	Index-wise statistics	Majority voting
RFA [36]	Euclidean distance	Geometric median

In this setup, the flow of the overall framework with Byzantines performing an attacking strategy, denoted by  $Attack(\cdot)$ , and the robust aggregator, denoted by  $AGG(\cdot)$  that is implemented at the server, is illustrated in Algorithm 1. In general, the attack  $Attack(\cdot)$  can be considered as a mapping

$$Attack(\cdot) : \mathcal{H}_t \rightarrow (\mathbf{m}_{i,t} \mid i \in \mathcal{K}_{mal}) \in \mathbb{R}^d, \quad (2)$$

where  $\mathcal{H}_t$  is referred to as history and includes all the available information to Byzantines until  $t$ .

**Adversary Model:** We assume the adversary controls up to  $k_m$  out of  $k$  total clients, called malicious clients. We assume that the number of malicious clients is less than the number of benign clients, i.e.,  $(k_m/k) < 0.5$ ; otherwise, no Byzantine-robust aggregator will be able to defeat poisoning attacks. Following the previous works [1], [2], [4], [14], [39], [48], we assume that the adversary can access the global model parameters broadcast in each epoch and can directly manipulate the gradients on malicious devices. Further, Byzantines can also compute the momentum of the benign clients. On the other hand, Byzantines form their attacks in an agnostic manner with respect to the aggregator. In other words, the Byzantines do not know the robust aggregator or the defence mechanism used by the PS. Hence, the attack should be universal; that is, it should be effective against all known defence mechanisms without any aggregator-specific calibration.

## II. PRELIMINARIES AND RELATED WORK

### A. Analyzing Existing Defence Methods

Various defence mechanisms against Byzantines have been introduced recently to ensure the learned model's reliability. Often the underlying defence mechanism is to detect Byzantines utilizing different measures and ignore their model update. However, some works directly sanitize each user's model update rather than filtering the attackers.

In a broad sense, we can classify Byzantine detection strategies into three main categories based on the identification measures used for outliers: geometric distance, index-wise statistics, and angular variance.

1) *Geometric distance:* In this section, we analyze the norm-based defences where robust aggregators consider the geometric distances to identify outliers.

**Multi Krum:** The underlying idea behind the Krum mechanism [6] is to identify where the benign vectors accumulate in close proximity. Under the assumption of  $k_m$  Byzantines, considered as outliers, the first step of the Krum is to form a set

### Algorithm 2 Robust aggregation with CC

---

```

1: Inputs:  $\tilde{\mathbf{m}}_t, \{\mathbf{m}_{i,t}\}_{i \in \mathcal{K}}, \tau$ 
2: for  $i = 1, \dots, k$  do in parallel
3:    $\tilde{\mathbf{m}}_{i,t} = f_{CC}(\mathbf{m}_{i,t} | \tilde{\mathbf{m}}_t, \tau)$ 
4:  $\tilde{\mathbf{m}}_t = \frac{1}{k} \sum_{i \in \mathcal{K}} \tilde{\mathbf{m}}_{i,t}$ 

```

---

of neighbouring nodes  $\mathcal{S}_i$ , for each vector  $\mathbf{m}_i$ , with cardinality  $k^* = k - k_m + 2$  such that

$$\mathcal{S}_i^* = \min_{\mathcal{S}, |\mathcal{S}|=k^*} \sum_{j \in \mathcal{S}} \|\mathbf{m}_i - \mathbf{m}_j\|^2. \quad (3)$$

Then, Krum identifies the vector  $\mathbf{m}_i$ , that has the minimum average distance  $d_i$  to vectors in its closest neighbourhood  $\mathcal{S}_i^*$  as the true center for the benign vectors, i.e.,

$$\operatorname{argmin}_{i \in \mathcal{K}} d_i = \sum_{j \in \mathcal{S}_i^*} \|\mathbf{m}_i - \mathbf{m}_j\|^2 \quad (4)$$

Multi-krum is built on the same principle but chooses  $n$  vectors instead of a single one and outputs their average.

**Centered Clipping (CC):** One of the major shortcomings of the robust aggregators that rely on outlier elimination is the assumption that the number of Byzantines is known in advance. Even under this assumption, such methods suffer from miss-classification of benign clients as outliers or under-utilization of benign models [2], [25]. Hence, in [24], the authors argue to utilize all the available model updates but first sanitize them. The underlying idea behind the CC is to perform sanitization by projecting model update  $\mathbf{m}$  into a ball with radius  $\tau$  and centered at reference model  $\tilde{\mathbf{m}}$ , accordingly, the clipping function  $f_{cc}(\cdot)$  can be formulated as

$$f_{CC}(\mathbf{m} | \tilde{\mathbf{m}}, \tau) = \tilde{\mathbf{m}} + \min \left\{ 1, \frac{\tau}{\|\tilde{\mathbf{m}} - \mathbf{m}\|} \right\} (\mathbf{m} - \tilde{\mathbf{m}}). \quad (5)$$

Further, they argue that by choosing the previous aggregate model update as the reference model for the current step, i.e.,  $\tilde{\mathbf{m}}_t = \tilde{\mathbf{m}}_{t-1}$ , it is possible to sanitize poisoned model updates successfully. However, in [54], the authors show that when Byzantines are not oblivious to  $\tilde{\mathbf{m}}_t$  and modify their adversarial perturbation accordingly, CC becomes ineffective. As we further discuss in section II-B, CC has certain other weaknesses.

**RFA:** is a geometric median-based robust aggregation method [36] such that given set of  $n$  vectors  $\{\mathbf{m}_1, \dots, \mathbf{m}_n\}$  the consensus model is solution,  $\mathbf{m}^*$ , of the following optimization problem;

$$RFA(\mathbf{m}_1, \dots, \mathbf{m}_n) = \operatorname{argmin}_{\mathbf{m}^*} \sum_{i=1}^n \|\mathbf{m}^* - \mathbf{m}_i\|_2. \quad (6)$$

It reduces the impact of the contaminated updates by approximating the geometric median in place of the weighted arithmetic mean, resulting in an aggregated global model update that looks robust to outliers.

2) *Index-wise statistics*: Numerous algorithms based on stochastic gradient descent (SGD) have been proposed to solve Eqn. 1 under these distributed optimization frameworks. Performing updates based on the mean of the local stochastic directions is the fundamental concept. On the other hand, there are prominent and interesting algorithms whose updates are not directly related to the mean of the local updates.

**SignSGD.** [3], [23] It lowers communication overheads by updating the parameters according to a majority vote of momentum signs. It also allows fault tolerance by employing majority voting. More formally, we can define SignSGD as;

$$\text{SignSGD}(\mathbf{m}_1, \dots, \mathbf{m}_k) = \text{sign}\left(\sum_i^k \text{sign}(\mathbf{m}_i)\right). \quad (7)$$

**CM** (coordinate-wise median) [52], employs the index-wise median of momentums to evaluate the mean of the local updates in order to ensure robustness against Byzantine workers.

$$\hat{\mathbf{m}} = CM(\mathbf{m}_1, \dots, \mathbf{m}_k) : \hat{\mathbf{m}}[j] = \text{median}(\mathbf{m}_1[j], \dots, \mathbf{m}_k[j]) \quad (8)$$

**TM** (Trimmed Mean) [52], is proposed as a more robust Byzantine resilient aggregator to CM by discarding some of the outlier indices and then taking the mean of the remaining ones. It offers less statistical error under the assumption that the number  $k_m$  of Byzantines is known.

In TM; for each coordinate,  $j$ , let  $S_j$  denote the ordered set formed by permuting the elements in set  $[n]$ , such that the order is determined by sorting the  $j$  coordinate values. We compute the average after discarding the  $k_m$  largest and smallest values; hence the name trimming [52].

$$[TM(\mathbf{m}_1, \dots, \mathbf{m}_n)]_j = \frac{1}{k - 2k_m} \sum_{i=k_{m+1}}^{k-k_{m-1}} [\mathbf{m}_{S_j(i)}]_j \quad (9)$$

Based on the variance and skewness of the various workers, the authors [52] bound the error rate that their method ensures. As such, the larger the variance and skewness, the higher the error rate the attacker can achieve. Nevertheless, regardless of the variance, Byzantine clients can steadily accumulate errors as long as staying close to the  $\bar{\mathbf{m}}$  [2], [14], [39].

**Bulyan** repeatedly employs TM and Multi-Krum to select client momentum to defend against Byzantine attacks. The underlying idea in Bulyan is that, with a single gradient dimension that is extremely large, a malicious gradient can stay near benign gradients and impede the global model's convergence [12].

**GAS** highlights that the existing defence mechanisms suffer from the curse of dimensionality and argues that it is possible to enhance the robustness of existing aggregators by dividing the whole update vector into  $p$  sub-vectors and performing aggregation for each sub-vector independently. The hyper-parameter  $p$  is chosen according to the size of the underlying NN architecture, and often larger values are employed for better robustness.

## B. Analyzing Existing Attack Methods

**ALIE:** [2] Traditional aggregators such as Krum [6], TM [52], and Bulyan [12] assume that the selected set of momentums will lie within a ball centered at the real mean within a radius, which is a function of the number of benign clients. The attacker in [2] utilizes index-wise mean ( $\bar{\mathbf{m}}$ ) and standard deviation ( $\bar{\sigma}$ ) vectors of the benign clients to induce small but consistent perturbations to the parameters. By keeping the momentum values close to  $\bar{\mathbf{m}}$ , ALIE can steadily achieve an accumulation of error while concealing itself as a benign client during training. To avoid detection and stay close to the center of the ball, ALIE scales  $\bar{\sigma}$  with a  $z$  parameter, which is calculated based on the numbers of benign and Byzantine clients. As such, let  $s$  be the minimal number  $s = \lfloor \frac{k}{2} + 1 \rfloor - k_m$  of benign clients that are required as *supporters*. The attacker will then use the properties of the normal distribution, specifically the cumulative standard normal function  $\phi(z)$ , and look for the maximum value of  $z$ , denoted by  $z^{max}$ , such that  $s$  benign clients will have a greater distance to the mean compared to the Byzantine clients, such that, those  $s$  clients are more likely to be classified as Byzantines. At a high level,  $z^{max}$  can be calculated as:

$$z^{max} = \max \left\{ z : \phi(z) < \frac{k - k_m - s}{k - k_m} \right\} \quad (10)$$

Ultimately,  $z^{max}$  is employed as a scaling parameter for the standard deviation to perturb the mean of the benign clients in set  $\mathcal{K}_b$ :

$$\mathbf{m}_i = \bar{\mathbf{m}} - z^{max} \bar{\sigma}, i \in \mathcal{K}_m, \quad (11)$$

where  $\mathcal{K}_m$  is the set of Byzantine clients. Each individual Byzantine client generates an attack with a momentum value near  $\bar{\mathbf{m}}$ , following (11).

**IPM:** [48] From the perspective of convergence analysis, the authors [48] highlight the required condition that the inner product between the benign gradient  $\bar{\mathbf{g}}$  and the output of the robust estimator should be positively aligned, i.e.,

$$\langle \bar{\mathbf{g}}, AGG(\mathbf{g}_i : i \in \mathcal{K}) \rangle \geq 0, \quad (12)$$

which ensures that the loss is steadily minimized over iterations. Hence, IPM generates poisoned model updates at each iteration with an objective that the condition in eqn (12) is not met. To this end, IPM chooses the benign gradient with the inverse sign,  $-\bar{\mathbf{g}}$ , as its base<sup>1</sup> for the attack and choose a proper scaling parameter  $z$  for imperceptibility so that the final version of the attack  $-z\bar{\mathbf{g}}$  is not easily spotted but hinders the convergence. One of the major drawbacks of IPM is being easily spotted by an angular investigation and the need for a large ratio of  $\frac{k_m}{k_b}$  actually to prevent eqn 12.

**Adaptive Optimized Attacks:** ALIE and IPM attacks utilize a fixed pre-determined scaling parameter throughout the training process. In [39], the authors utilize the ALIE and

<sup>1</sup>When the aggregation is performed over momentum terms the attack is performed as  $-z\bar{\mathbf{m}}$ .

IPM framework to obtain the base form of the perturbation. However, instead of fixed scaling parameter  $z$ , they adaptively change it by solving an optimization problem with the objective of maximizing  $z$  under certain geometric distance based imperceptibility constraints at each iteration.

### III. SPARSE BYZANTINE ATTACKS

This section highlights the key design aspects of our sparse Byzantine attacks and provides the intuition behind each aspect. Before introducing our proposed Byzantine attack, we revisit the ALIE attack, which will be the base for our design due to certain important features we identify.

#### A. Revisiting ALIE attack from the defence perspective

The key design objective of the ALIE is to find the adversarial model update values,  $\mathbf{m}_{adv}$ , such that: 1) the adversarial values are not statistical outliers, 2) the adversarial values strong enough to shift distribution. To achieve this target, ALIE utilizes the index-wise statistics, i.e.,

$$\mathbf{m}_{adv} = \bar{\mathbf{m}} - z\bar{\sigma} \quad (13)$$

where  $\bar{\sigma}$  is the vector of index-wise standard deviation and  $z^{max}$  is the scaling factor adjusted according to the Byzantine ratio for the imperceptibility. From the construction, one can easily observe how ALIE can escape from index-wise statistical examinations and the corresponding defence methods such as TM.

Further, as discussed in [2], ALIE is also effective against defence mechanisms that utilize geometric distance as a metric to identify outliers, such as Krum, where the aggregation rule selects a model update from the available model updates, including both clean and Byzantine updates, which achieves the minimum value of the neighbourhood distance measure.<sup>2</sup> We emphasize the following observation: the structure of both Krum and TM defence mechanisms are based on outlier elimination, and even if they successfully detect Byzantines, they also falsely classify some benign updates as outliers, which is more frequent when the data is distributed in a non-iid fashion. In [25], it has been further shown that this type of defence mechanism deteriorates the performance even when there are no Byzantines or Byzantines just mimicking the benign clients as an attack.

Therefore, as an alternative, sanitization-based defences first sanitize all the model updates to minimize the impact of Byzantines and then perform an aggregation over all the sanitized models in order to avoid falsely discarding the true benign clients. Indeed, as we later numerically illustrate through extensive simulations, CC framework, which sanitizes models through vector-wise clipping, is quite effective against the ALIE attack. However, in [54], the authors also identify certain limitations of the CC. To be more precise, CC only scales the deviation from the reference model (aggregate

<sup>2</sup>Multi-Krum relies on the same measurement; however, instead of performing an aggregation rule that directly chooses a representative model, Multi-Krum first eliminates the outliers and then performs averaging as an aggregation rule for the remaining ones.

TABLE III: ALIE attack with different scaling values against CC aggregator on IID CIFAR-10 dataset trained on Resnet-20 architecture with  $k = 25$  and  $k_m = 5$ .

$z$	Angle	Cos. Sim.	Norm	Accuracy %
0.25	92	0.82	0.4	82
0.5	88	0.93	0.7	66
1	77	0.97	1.2	50
1.5	76	0.98	1.7	50

momentum in the previous round), and thus, angular invariant to the direction of the perturbation. To better illustrate, when a Byzantine client follows ALIE strategy, it sends  $\bar{\mathbf{m}} - z\bar{\sigma}$  as a poisoned model update, and CC mechanism first measures the drift with respect to the reference update  $\bar{\mathbf{m}}_t$ ,

$$\Delta_t^{ref} = \bar{\mathbf{m}}_t - \bar{\mathbf{m}}_t + z\bar{\sigma}_t, \quad (14)$$

then clip the drift  $\Delta_t^{ref}$  if its norm is larger than  $\tau$ , i.e.,

$$\tilde{\Delta}_t^{ref} = \min \left\{ 1, \frac{\tau}{\|\Delta_t^{ref}\|} \right\} \Delta_t^{ref}, \quad (15)$$

which we refer to as effective perturbation, and as one can observe, the clipping only depends on the norm of  $\Delta_t^{ref}$ . Hence, when ALIE utilizes a larger scaling parameter  $z$ , CC can detect and clip the attack. However, such clipping does not necessarily change the direction of the adversarial perturbation nor prevents their correlation over time, which enhances the time-coupled nature of the ALIE, as illustrated in [54], and plays a key role in diverging the model.

To clarify the discussion above, we conduct an experiment where we employ ALIE with scaling parameters  $z \in \{0.25, 0.5, 1, 1.5\}$  and CC with  $\tau = 1$  as a robust aggregator, and then for each scaling value we measure the average norm of the drift  $\|\Delta_t^{ref}\|$ , the expected angle between the effective perturbation  $\tilde{\Delta}_t^{ref}$ ,  $\angle(\tilde{\Delta}_t^{ref}, \bar{\mathbf{m}}_t)$ , and the reference update  $\bar{\mathbf{m}}_t$ , and finally temporal correlation on the effective perturbation, that is, the cosine similarity between the consecutive effective perturbations,  $\cos(\tilde{\Delta}_t^{ref}, \tilde{\Delta}_{t-1}^{ref})$ . The results are illustrated in Table III, which clearly demonstrates that being clipped by the CC does not imply being sanitized properly. To be more precise, as the scaling parameter  $z$  is increased, CC starts clipping the perturbation  $\Delta_t^{ref}$ , as the norm goes beyond  $\tau = 1$ . But under such clipping, the orthogonality of the perturbation is still preserved, and as highlighted by [54], this is quite important for derailing the model. The key observation here is that as the scaling parameter  $z$  increases, the time-coupled nature of the ALIE, measured through cosine similarity, becomes more and more visible. Thus, we conclude that the CC strategy gives a false sense of security against ALIE, and its performance highly depends on the choice of  $z$ .

Next, we move our focus to the robust aggregators that utilize index-wise outlier investigation, such as CM and TM, and analyze their performance with respect to the scaling parameter  $z \in \{0.25, 0.5, 1, 1.5, 2\}$ . For the analysis, we again consider the same simulation setup, but this time we measure

the final test accuracy and the escape ratio, which is the average percentage of the indices where the Byzantine model evades the index-wise statistical outlier investigation; in the case of CM, this means the median is equal to the poisoned model. The results are exhibited in Table IV. One immediate observation from the results is that, up to a certain level in the experiment, the best performance is observed when  $z = 0.5$ , and increasing the value of  $z$  may lead the attack to be more visible but also have a stronger perturbation. In ALIE, the authors have stated, "We would like to induce directed small changes to many parameters, instead of large changes to a few", whereas we argue both can be performed at the same time.

**Our key design aspect:** Based on the aforementioned discussion and observations, we argue that the ultimate objective should not always be being invisible, and sometimes, the attack can seek a balance between being invisible and having a stronger perturbation. The more interesting observation, which inspired our proposed Byzantine design, is that in terms of the final test accuracy, effectively attacking only a certain portion of the indices but with a higher perturbation might be more effective than attacking all indices with relatively smaller perturbation. Hence, we utilize a hybrid design that combines two different types of attacks, one being more conservative and imperceptible and the other being more aggressive but less imperceptible, which can be simply obtained by choosing two different scaling  $z$  values. Later in section III-B, we further explain how these two sub-attacks are generated and combined to form the final version of our attack.

Until this point, we have shown that when a sufficiently large  $z$  value is chosen, both CC and index-wise defence methods, TM and CM, are not effective against ALIE. We then further discuss why larger  $z$  is not desired from the geometric-distance based defence strategies like Bulyan and Krum. To visualize the discussion, we again follow the same simulation setup, with Bulyan and Krum as the robust aggregators, and the results are illustrated in Table V. We emphasize that, unlike the previous robust aggregators, with Bulyan and Krum, we observe a drastic change in the accuracy when the value of  $z$  goes beyond a certain level; in our simulation, it appears at  $z = 1.5$ . In contrast to our previous observations, in the case of geometric distance-based defences, when Byzantines are spotted, they immediately become ineffective since, unlike index-wise investigation, these defences consider all indices, either Byzantine or benign. This observation further supports our claim regarding the need for a hybrid attack. To be more precise, by attacking aggressively, with larger  $z$ , to only certain indices rather than all, the imperceptibility of the attack against geometric-distance based investigation can be preserved. In the next section, we formalize the structure of the proposed hybrid attack based on the discussion above.

### B. Our Hybrid Sparse Attack Design

In our *sparse Byzantine attack* design, our objective is to introduce a framework that can escape from both index-wise and Euclidean distance-based sanitization methods simultane-

TABLE IV: Index-wise escape ratios for the ALIE attack with different  $z$  scales on the CM and TM aggregators. Acc. corresponds to IID CIFAR-10 test accuracy trained on Resnet-20 with  $k = 25$  and  $k_m = 5$ .

$z$	CM		TM	
	Escape ratio (%)	Acc.	Escape ratio (%)	Acc.
0.25	66	45.43	99.9	72.7
0.5	14	39.4	98	36.35
1	0	48.3	63	47.9
1.5	0	47.5	25	45.1
2	0	49.3	7.5	42.9

TABLE V: Escape ratios for the Multi-Krum and Bulyan for ALIE attack. Acc. corresponds to IID CIFAR-10 test accuracy trained on Resnet-20 with  $k = 25$  and  $k_m = 5$ .

$z / \text{AGGR}$	Krum			Bulyan		
	Client %	Indices %	Acc.	Client %	Indices %	Acc.
0.25	100	-	55.75	100	73	47.13
0.5	100	-	45.15	100	60	47.43
1	100	-	45.32	100	29	32.79
1.5	0	-	87.4	0	0	86.54

ously. In the previous section, we highlighted that although index-wise statistically imperceptible attacks, e.g., ALIE, are effective against index-wise defence strategies, such as TM, thanks to their time coupling nature, they often become impotent against Euclidean distance-based defence mechanisms, such as CC.

Based on these observations, we propose to utilize a hybrid byzantine attack that can be decomposed into two parts; each part targets a different type of defence mechanism, i.e.,

$$\Delta = \Delta_1 + \Delta_2, \quad (16)$$

where  $\Delta_1$  is formed by following a similar strategy to ALIE, that is, the poisoned update  $\bar{\mathbf{m}}_t + \Delta_{t,1}$  is statistically imperceptible to index-wise inspection, with respect to the  $\bar{\mathbf{m}}_t$ , i.e.,

$$\bar{\mathbf{m}}_t[i] + \Delta_{t,1}[i] \in (\bar{\mathbf{m}}_t[i] - \alpha\sigma_{i,t}, \bar{\mathbf{m}}_t[i] + \alpha\sigma_{i,t}), \quad (17)$$

However, while still being bounded, adversarial perturbation  $\Delta_{t,1}$  accumulates over time to inhibit the convergence.

On the other hand, for  $\Delta_{2,t}$ , we focus on an Euclidean distance-based constraint rather than the index-wise constraint given in eqn. (17), i.e.,

$$\|\Delta_{2,t}\|_2 \ll \|\bar{\mathbf{m}}_t\|_2. \quad (18)$$

Hence, when  $\Delta_{2,t}$  is employed alone, it can easily escape defences that utilize geometric distance as an anomaly metric, and further, it cannot be detected with angular inspection as well.

The key challenge here is how to preserve the aforementioned features of each attack when they are linearly combined to form the final adversarial perturbation  $\Delta_t$ . To this end, we consider the following strategy that let  $\mathcal{M}_1 \cup \mathcal{M}_2 = [d]$  and  $\mathcal{M}_1 \cap \mathcal{M}_2 = \emptyset$ , then if  $i \in \mathcal{M}_1$   $\Delta_{2,t}[i] = 0$  and  $\Delta_{1,t}[i] = 0$ , otherwise. Further, when  $|\mathcal{M}_1| \ll d$ , we can assure eqn

(17) for most of the indices, hence still achieving index-wise imperceptibility. Accordingly, we generate the Byzantine perturbation  $\Delta_t$  in the following way: We first generate a sparse binary mask  $\mathbf{c} \in C \triangleq \{0, 1\}^d$  (later we further explain how to obtain such mask), and then generate a pair of scaling parameters  $(z_1, z_2)$  which are used to form the adversarial perturbation in the following way

$$\Delta_t = (z_1(1 - \mathbf{c}) + z_2\mathbf{c}) \odot \sigma_t, \quad (19)$$

and then the poisoned model is simply obtained by adding  $\Delta_t$  to the benign update  $\tilde{\mathbf{m}}_t$ . Hence, the key design problem regarding our sparse Byzantine attack is generating the sparsity mask  $\mathbf{c}$  and finding the proper pair of scaling values  $(z_1, z_2)$ . Assume that  $\mathbf{c}$  is known for now. Since from the construction, we expect that the part corresponding to  $\Delta_{t,1} = z_1(1 - \mathbf{c})$  to be imperceptible against index-wise investigation, we set  $z_1 = z_1^{max}$ , that is the maximum scaling value obtained with respect to the Byzantine ratio according to scheme introduced in ALIE.

Once  $\mathbf{c}$  and  $z_1$  are fixed, the challenge boils down to selecting the appropriate value for  $z_2$ . We have already highlighted the trade-off between the imperceptibility and the strength of perturbation; thus, choosing an arbitrarily large  $z_2$  value may not be effective. Accordingly, we have utilize Chebyshev's inequality as a guide for limiting the value of  $z_2$ , that is, Chebyshev's inequality states

$$Pr(|\tilde{\mathbf{m}}[i] - \mathbf{m}[i]| > z_2\sigma[i]) \leq \frac{1}{z_2^2}, \quad (20)$$

hence, we argue that any choice of  $z_2 > \sqrt{2} \approx 1.5$  may make the perturbation highly visible from the statistical perspective, indeed this argument is highly aligned with our initial numerical experiments, in which we investigate the visibility of the perturbation as illustrated in Table IV and Table V with respect to various values of  $z$ , where we observe scaling  $z$  beyond 1.5 make the attack to be easily spotted by known defence mechanisms. Here, we also note that rather than fixing  $z_1 = z_1^{max}$ , it is possible to seek an adaptive strategy such that the optimal value of  $z_1$  is reset at each iteration with respect to the benign updates  $\mathbf{M}_t \triangleq \{\mathbf{m}_{i,t};\}_{i \in \mathcal{K}_b}$ , as previously argued in [39]. The overall hybrid Sparse Byzantine attack mechanism is illustrated in Algorithm 3.

### C. Generating Sparse Mask

In the previous part, we explained how one can generate a Byzantine attack for a given sparsity mask  $\mathbf{c}$ . In this section, investigate how to generate a sparsity mask  $\mathbf{c}$ . The vanilla approach to generate a sparsity mask is random sparsity; that is, for a given sparsity ratio  $\delta$ , we can randomly generate a binary value for each index i.e., for each  $i \in [d]$ ,

$$\mathbf{c}[i] = \begin{cases} 0, & \text{if } w.p. \delta \\ 1, & \text{if } w.p. 1 - \delta \end{cases}. \quad (21)$$

The previous studies on neural network pruning have shown that, for a moderate sparsity level  $\delta$ , random sub-networks often achieve the performance of dense networks [16]. Thus,

---

### Algorithm 3 Hybrid Sparse Attack

---

```

1: for t=1...T do
2:   if t == 1 then
3:     Initialization Inputs: Colluded dataset  $D_{col}$ , target sparsity  $\delta$ , pruning policy  $\Pi$ , initial model weights  $\theta_0 \in \mathbb{R}^d$ 
4:     Initialization Phase:
5:     Generate mask  $\mathbf{c}$  for given  $D_{col}, \Pi, \theta_0, \delta$ 
6:     Inputs: Benign updates  $\mathbf{M}_t$ , benign statistics  $(\sigma_t, \tilde{\mathbf{m}}_t)$ ,  $z_1^{max}, z_2^{max}$ 
7:     Generate pair of scaling parameters  $(z_1^{(t)}, z_2^{(t)})$ 
8:     Option 1: Fixed policy
9:     Use fixed scaling  $z_1^{(t)} = z_1^{max}$  and  $z_2^{(t)} = z_2^{max}$ 
10:    Option 2: Semi-adaptive policy
11:    Use fixed  $z_2^{(t)} = z_2^{max}$  and optimize  $z_1^{(t)}$  acc. MinSum Policy [39]
12:    Generate perturbation:  $\Delta_t = (z_1^{(t)}(1 - \mathbf{c}) + z_2^{(t)}\mathbf{c}) \odot \sigma_t$ 
13:    Poisoned model:  $\mathbf{m}_{adv} = \tilde{\mathbf{m}}_t - \Delta_t$ 

```

---

by establishing an analogy between a sparse attack and a sparse network, we argue that a random sparsity pattern, that is, the number of NN weights being attacked at each layer is proportional to the dimension of the corresponding layer, would be a good candidate for the sparse Byzantine attack. Indeed, as we later demonstrate, random sparsity mask works well against various defence mechanisms.

However, regarding the robustness of the trained model, the impact of each layer may not be identical, and from the network pruning perspective, one may need to assign a different sparsity ratio to each layer. To clarify, having a set of  $l$  layers  $\mathcal{L} = [l]$ , one may consider a different sparsity ratio  $\delta_l$  that satisfies the overall sparsity constraint  $\frac{\sum_{i \in \mathcal{L}} \delta_l d_l}{d} = \delta$ . In the literature, there are different approaches to distribute the sparsity among different layers; for instance, in [13], the authors utilize *Erdos-Renyi-Kernel (ERK)* formulation. Another important aspect often emphasized in the literature on sparse networks is certain sensitive layers, which we further clarify next, being excluded from the network pruning since these parts of the NN model are highly sensitive [9], [42]. Therefore, from the attack perspective, we argue that we should attack these sensitive layers particularly. Accordingly, we make all the corresponding locations in  $\mathbf{c}$  have a value of 1 and consider the sparsity ratio  $\delta$  for the remaining layers.

We remark that the approaches or rules mentioned above *omniscient to target dataset* and do not induce a high *computational complexity*. On the other hand, it has been known that, in high-sparsity regimes, randomly generated sub-networks do not perform well. Equivalently, if we want to design an attack with a higher sparsity pattern, the randomly generated  $\mathbf{c}$  may not be a good option. Therefore, in that case, we can further utilize the small portion of the training data, that is, the data gathered by the colluding Byzantines, and perform network pruning to identify those important weights to be attacked. Further discussions on the performance of the aforementioned approaches, as well as different sparsity ratios, will be presented in the next section. Further, later in section III-C1, we revisit some of the network pruning strategies,

which work well with limited or no data, to form our sparse attack. From the design perspective, if one aims to make the attack even more imperceptible with higher sparsity, then we numerically show that the use of a network pruning strategy has a clear advantage compared to the randomly generated sparsity.

1) *Sparsity with Network Pruning*: The overall objective of NN pruning is to find a small subset of NN parameters  $\mathcal{M}$  with a size of  $\kappa \ll d$  such that the NN model with only the subset of the parameters  $\theta_{\mathcal{M}}$  is sufficient to achieve a certain loss over the given dataset  $D$ . Formally speaking, the objective can be formulated as

$$\begin{aligned} \min_{\mathbf{c}, \theta} F(\mathbf{c} \odot \theta; D) &= \frac{1}{|D|} \sum_{\zeta \in D} f(\mathbf{c} \odot \theta; \zeta) \\ \text{s.t. : } \|\mathbf{c}\|_0 &\leq \kappa \text{ and } \theta \in \mathbb{R}^d. \end{aligned} \quad (22)$$

In our work, we mainly focus on NN pruning strategies that are performed with a limited dataset since the Byzantines may have access to a limited number of data samples to form a sparsity pattern. In SNIP [29], the authors highlight that, for a given  $\theta$ , the additional loss incurred due to the pruning of the  $i^{\text{th}}$  weight, i.e.,

$$\Delta F_i = F(\mathbf{1} \odot \theta; D) - F((\mathbf{1} - \mathbf{e}_i) \odot \theta; D) \quad (23)$$

where  $\mathbf{e}_i$  is a one-hot vector where the  $i^{\text{th}}$  value is one and zeros everywhere except the  $i^{\text{th}}$  index. It can be approximated by gradient with respect to the  $\mathbf{c}$ , such that,

$$\begin{aligned} \Delta F_i &\approx \left. \frac{\partial F(\mathbf{c} \odot \theta; D)}{\partial c_i} \right|_{\mathbf{c}=\mathbf{1}} = \\ &\lim_{\delta \rightarrow 0} \left. \frac{F(\mathbf{c} \odot \theta; D) - F((\mathbf{c} - \delta \mathbf{e}_i) \odot \theta; D)}{\delta} \right|_{\mathbf{c}=\mathbf{1}}. \end{aligned} \quad (24)$$

The term above implies a directional derivative, a sparse direction, and thus can be simply written in the following form:

$$\theta_i \frac{\partial F(\theta; D)}{\partial \theta_i}. \quad (25)$$

Hence, SNIP concludes that  $s_i \triangleq |\theta_i \frac{\partial F(\theta; D)}{\partial \theta_i}|$  can be used as a salience measure for the connection sensitivity. Though building on the same idea, FORCE [9] argues for measuring the connection sensitivity *after* the pruning rather than before the pruning. To be more specific, FORCE examines the gradient for the foresight sparse model, i.e.,

$$\left. \frac{\partial F(\mathbf{c} \odot \theta; D)}{\partial \mathbf{c}} \right|_{\mathbf{c}=\hat{\mathbf{c}}}, \|\hat{\mathbf{c}}\|_0 = \kappa, \hat{\mathbf{c}} \in \mathcal{C} \quad (26)$$

Accordingly, FORCE searches for the binary sparse mask  $\mathbf{c}$  that maximize the following salience measure:

$$S(\theta, \mathbf{c}) = \sum_{i: \mathbf{c}[i]=1} \underbrace{|\theta \odot \nabla F(\mathbf{c} \odot \theta; D)|}_{s(\theta, \mathbf{c})}[i] \quad (27)$$

where  $\nabla F(\mathbf{c} \odot \theta; D) = \left( \frac{\partial F(\bar{\theta}; D)}{\partial \bar{\theta}} \right)_{\mathbf{c}}$ ,  $\bar{\theta} = \mathbf{c} \odot \theta$ , from equation (5) in [9]. However, such a strategy that measures connection sensitivity after pruning is practically not feasible due to its combinatorial complexity; that is, ideally, we need

to compute the salience for all possible  $\binom{d}{\kappa}$  sparsity patterns. To mitigate the combinatorial complexity, FORCE argues to perform pruning in an iterative manner, under the assumption that the change of the gradient can be neglected, rather than checking each possible sparsity pattern individually; for the details, refer to [9].

In our design, we utilize the FORCE framework since it does not require the whole dataset, which is aligned with our problem setup, where Byzantines can access a small portion of the dataset. Although, there is a strong analogy between NN pruning and sparse Byzantine attacks, when we implement the FORCE framework for high sparsity regime, such as  $\delta \leq 1\%$ , we observe that non-sparse positions are accumulated in certain layers of the network, namely early convolutional layers and penultimate fully connected layer on the CNN architectures. To better visualise, we plot the percentage of the remaining (non-pruned) weights for each layer of the ResNet Architecture after pruning with FORCE, which is shown in Fig. 1 as the colour orange. From the Byzantine perspective, targeting only certain layers may not be effective, especially when the employed robust aggregator performs a layer-wise defence investigation [30], [43]. Therefore, we modify the FORCE framework with certain layer-wise sparsity constraints so that the corresponding attack is more homogeneously distributed among the layers; in other words, we aim to prevent certain layers from being overemphasized. Accordingly, we introduce the term  $\delta_{max}$  to impose that the sparsity ratio of a layer cannot be larger than  $\delta_{max}$ . Our experiments show that pruning methods often overemphasize certain layers, particularly the penultimate FC layer, as illustrated in Fig. 1. Hence, we argue that imposing constraints for these particular layers is often sufficient for our purpose. The sparsity pattern obtained by setting  $\delta_{FC}^{max} = 0.25$  is illustrated in Fig. 1 as the colour blue, where we observe while the penultimate FC layer becomes more sparse the number of non-sparse positions in early convolutional layers increases.

## IV. NUMERICAL RESULTS

### A. Simulation Setup

For the simulation setup, we consider a synchronous and centralized FL framework with  $k=25$  participating clients. We set the Byzantine ratio  $\gamma = 0.2$ , i.e.,  $k_m=5$  clients are malicious, which is the common scenario in the literature [24], [54]. For the training, we follow a similar setup as in [24], [54], where we train our neural networks for 100 epochs with a local batch size of 32 and an initial learning rate of  $\eta = 0.1$ , which is reduced at epoch 75 by a factor of 0.1. In all the simulations, we utilize local momentum with  $\beta = 0.9$  since the use of local momentum reduces the variance and enhances the robustness against Byzantines.

1) *Datasets and Networks*: For the image classification task, we consider MNIST [28], FMNIST [46] and CIFAR-10 [27] datasets and train them with a 2-layer MLP, 2-



TABLE VI: Final test accuracy results of training ResNet-20 architecture with Cifar-10 dataset distributed IID over  $k = 25$  client  $k_m = 5$  of them being malicious. The training is performed over 100 epochs and repeated for 8 different aggregation mechanisms and under 8 different Byzantine attack strategies. The reported results are obtained by averaging 3 number of independent trials. We use **blue**, **red** and **green** to highlight the best results for fixed policy attacks, ALIE, Bit Flip, IPM, Label Flip, ROP dynamically optimized attacks, Min-Sum, Min-Max and proposed sparse hybrid attack variations with different sparsity constraint  $\delta$ , respectively, and we underline the best attack result against each defence mechanism.

Method	Bulyan	CC	CM	M-Krum	RFA	TM	GAS-KRUM	GAS-Bulyan
No ATK	87.63 ± 0.96	87.42 ± 0.45	88.03 ± 0.14	89.24 ± 0.67	88.2 ± 0.31	87.76 ± 0.37	87.7 ± 0.31	87.58 ± 0.41
ALIE	47.13 ± 16.1	80.73 ± 1.41	<b>45.09 ± 9.35</b>	<b>55.76 ± 13.78</b>	<u>32.26 ± 16.08</u>	72.78 ± 2.49	80.96 ± 0.92	81.06 ± 0.62
Bit Flip	86.18 ± 0.57	82.25 ± 0.66	80.86 ± 0.78	87.82 ± 0.31	87.5 ± 0.65	80.08 ± 0.88	86.52 ± 0.49	86.79 ± 0.84
IPM	70.01 ± 0.88	85.85 ± 0.33	54.52 ± 0.75	83.79 ± 0.11	66.36 ± 0.67	84.9 ± 0.1	85.26 ± 0.17	85.63 ± 0.32
Label Flip	85.78 ± 0.3	86.38 ± 0.55	79.89 ± 0.14	87.68 ± 0.14	86.28 ± 0.08	78.51 ± 0.26	87.11 ± 0.69	86.88 ± 0.63
ROP	<b>41.45 ± 1.98</b>	<b>47.38 ± 0.9</b>	79.03 ± 0.4	88.22 ± 0.5	43.25 ± 2.23	<b>62.72 ± 1.28</b>	<b>61.97 ± 1.57</b>	<b>63.55 ± 0.7</b>
<b>Best Attack *</b>	41.45 ± 1.98	47.38 ± 0.9	45.09 ± 9.35	55.76 ± 13.78	32.26 ± 16.08	62.72 ± 1.28	61.97 ± 1.57	63.55 ± 0.7
Min-Sum	<b>41.13 ± 0.51</b>	55.46 ± 5.21	<b>47.6 ± 0.37</b>	<b>55.12 ± 1.32</b>	49.4 ± 8.64	47.48 ± 7.44	55.12 ± 3.03	<b>49.85 ± 11.81</b>
Min-Max	67.17 ± 4.44	<b>40.32 ± 7.81</b>	47.97 ± 1.83	61.59 ± 11.95	<b>48.7 ± 2.75</b>	<b>42.87 ± 6.23</b>	<b>47.09 ± 3.93</b>	86.6 ± 0.19
$\Pi_r(\delta = 5 \times 10^{-3})$	42.98 ± 17.99	79.27 ± 0.4	39.97 ± 16.02	54.87 ± 5.29	42.67 ± 6.28	70.58 ± 1.26	78.93 ± 0.96	78.46 ± 1.29
$\Pi_r(\delta = 5 \times 10^{-2})$	47.62 ± 3.08	75.08 ± 0.76	45.94 ± 5.94	14.14 ± 2.01	48.41 ± 11.4	70.16 ± 1.93	75.85 ± 0.58	75.7 ± 1.3
$\Pi_r(\delta = 2 \times 10^{-1})$	40.25 ± 0.5	41.62 ± 2.5	49.27 ± 8.52	12.1 ± 0.68	59.43 ± 0.62	61.9 ± 2.36	65.03 ± 1.28	66.26 ± 2.17
$\Pi_r(\delta = 5 \times 10^{-1})$	28.17 ± 1.86	46.84 ± 2.76	42.13 ± 6.49	<b>11.4 ± 1.23</b>	47.82 ± 5.88	40.02 ± 5.52	48.29 ± 0.79	86.83 ± 0.53
$\Pi_r^+(\delta = 5 \times 10^{-3})$	37.85 ± 10.49	48.91 ± 20.78	45.5 ± 9.69	30.08 ± 11.79	45.21 ± 5.61	63.66 ± 11.99	80.49 ± 0.31	79.04 ± 1.24
$\Pi_r^+(\delta = 5 \times 10^{-2})$	37.53 ± 5.3	50.14 ± 9.82	49.62 ± 9.44	14.23 ± 0.7	50.03 ± 1.94	61.39 ± 5.87	72.17 ± 1.1	73.14 ± 1.1
$\Pi_r^+(\delta = 2 \times 10^{-1})$	26.84 ± 1.21	43.04 ± 1.28	45.47 ± 5.19	14.75 ± 1.39	39.31 ± 10.38	46.25 ± 2.4	61.51 ± 6.0	60.67 ± 4.96
$\Pi_r^+(\delta = 5 \times 10^{-1})$	27.59 ± 2.56	38.86 ± 0.63	43.1 ± 10.64	11.46 ± 0.9	<b>36.84 ± 2.91</b>	31.34 ± 9.72	<b>39.34 ± 7.34</b>	86.15 ± 0.09
$\Pi_{lr}(\delta = 5 \times 10^{-3})$	44.55 ± 17.42	79.24 ± 0.3	36.72 ± 1.78	54.74 ± 4.75	52.97 ± 3.84	71.66 ± 3.55	81.23 ± 1.03	80.2 ± 0.89
$\Pi_{lr}(\delta = 5 \times 10^{-2})$	53.15 ± 3.91	75.44 ± 1.95	36.28 ± 5.56	26.7 ± 11.08	53.92 ± 5.87	67.88 ± 2.93	74.24 ± 2.61	74.69 ± 0.7
$\Pi_{lr}(\delta = 2 \times 10^{-1})$	36.27 ± 2.55	40.99 ± 2.14	50.32 ± 5.19	13.32 ± 1.89	59.37 ± 2.0	62.09 ± 2.91	64.92 ± 3.19	61.87 ± 3.6
$\Pi_{lr}(\delta = 5 \times 10^{-1})$	26.33 ± 2.59	37.52 ± 8.25	50.58 ± 3.41	13.27 ± 3.62	48.44 ± 5.17	39.66 ± 1.44	48.03 ± 1.78	86.82 ± 0.45
$\Pi_{lr}^+(\delta = 5 \times 10^{-3})$	32.78 ± 4.38	74.71 ± 5.22	45.29 ± 6.27	13.83 ± 0.96	45.58 ± 4.33	56.61 ± 18.7	78.89 ± 1.23	77.27 ± 1.82
$\Pi_{lr}^+(\delta = 5 \times 10^{-2})$	32.03 ± 5.44	45.11 ± 2.04	35.94 ± 7.81	16.5 ± 2.91	56.84 ± 2.83	58.99 ± 7.14	73.16 ± 0.64	69.88 ± 1.91
$\Pi_{lr}^+(\delta = 2 \times 10^{-1})$	<b>26.03 ± 3.01</b>	34.33 ± 7.28	48.05 ± 1.81	17.69 ± 1.69	46.71 ± 4.82	42.3 ± 7.16	58.74 ± 6.04	56.08 ± 8.72
$\Pi_{lr}^+(\delta = 5 \times 10^{-1})$	26.27 ± 3.35	37.63 ± 7.02	45.28 ± 3.51	13.51 ± 1.92	42.7 ± 2.77	<b>30.57 ± 0.49</b>	39.18 ± 2.52	87.0 ± 0.38
$\Pi_{ERK}^+(\delta = 5 \times 10^{-3})$	26.66 ± 1.09	40.96 ± 5.2	44.35 ± 13.51	16.26 ± 1.34	45.31 ± 12.67	72.06 ± 0.6	77.97 ± 0.55	73.33 ± 1.58
$\Pi_{ERK}^+(\delta = 5 \times 10^{-2})$	57.42 ± 0.43	65.18 ± 9.33	47.09 ± 4.81	61.39 ± 7.84	69.86 ± 0.67	62.86 ± 10.84	70.8 ± 3.51	73.59 ± 1.02
$\Pi_{ERK}^+(\delta = 2 \times 10^{-1})$	58.49 ± 0.9	50.74 ± 11.08	55.35 ± 1.73	56.7 ± 6.78	65.59 ± 1.28	58.29 ± 4.5	61.13 ± 4.51	71.46 ± 2.1
$\Pi_{ERK}^+(\delta = 5 \times 10^{-1})$	85.32 ± 0.74	52.6 ± 10.18	50.1 ± 2.66	55.0 ± 15.12	59.69 ± 1.55	49.23 ± 2.96	51.88 ± 2.74	86.32 ± 0.21
$\Pi_r^+(\delta = 5 \times 10^{-3})$	40.65 ± 1.71	39.61 ± 3.61	39.46 ± 9.21	15.47 ± 1.16	52.79 ± 10.89	53.53 ± 16.59	74.55 ± 3.95	74.82 ± 3.34
$\Pi_r^+(\delta = 5 \times 10^{-3}, \delta_{FC}^{max} = 0.25)$	31.34 ± 2.67	<b>33.92 ± 2.88</b>	<b>35.71 ± 4.46</b>	16.33 ± 2.06	42.7 ± 10.29	33.44 ± 3.26	59.51 ± 17.81	<b>52.54 ± 8.34</b>
$\Pi_r^+(\delta = 1 \times 10^{-2}, \delta_{FC}^{max} = 0.25)$	28.39 ± 1.89	38.69 ± 0.99	42.27 ± 17.84	16.33 ± 2.06	39.9 ± 9.44	47.54 ± 6.68	67.75 ± 8.23	59.34 ± 9.52

layer convolutional neural network (CNN), and Resnet-20 [22] architectures, respectively.

We consider two scenarios where we distribute the data among the clients in IID and non-IID manners, respectively. In the IID scenario, we distribute the training data homogeneously among the clients with respect to their labels. In the non-IID scenario, similar to previous works [20], [40], [44], [51], the dataset is divided among the clients according to Dirichlet distribution [32] with parameter  $\alpha$ , denoted by  $\text{Dir}(\alpha)$ , where  $\alpha$  parameter controls the skewness of the probability distribution with respect to the class labels. In our experiments, we set  $\alpha = 1$ , which is argued to be valid to simulate practical scenarios.

2) *Aggregators*: We consider Bulyan, CC, CM, MultiKrum, RFA, SignSGD, and TM for the robust aggregators. We also employ GAS with Bulyan and MultiKrum since they are the best-performing base aggregators with the GAS framework [30]. For CC, we employ a fixed ball radius of  $\tau = 1$  since a higher radius is more susceptible to Byzantine attacks [37], [54], and lower  $\tau$  performs suboptimally in non-IID settings [54] and the number of clipping iterations to  $l = 1$ . For GAS, we set  $p = 1000$  on ResNet-20 and 2-Layer CNN, while on 2-layer MLP, we set  $p = 100$  due to the smaller network size. Our  $p$  values are proportional to the best  $p$  parameter that

authors employed in their works for their NN size [30]. For SignSGD, we employ an initial learning rate of 0.01, which makes learning more stable.

3) *Attacks*:: For non-omniscient attacks, we consider the bit-flip and label-flip [5], [17] attacks. In the bit-flip attack, Byzantine clients flip the signs of their own gradient values, whereas, in the label-flip attack, Byzantine clients flip the label of a sample by subtracting it from the total number of image classes in the dataset. For the omniscient model poisoning attacks, we consider ALIE [2], IPM [48], and ROP [54]. In ROP, we employ the original parameter values given in [54]. For IPM, previous works have considered different  $z$  values, i.e., in [24]  $z = 0.1$  and in [54]  $z = 0.2$ . In our early experiments, we tried different  $z$  values, including the previously used ones  $z = 0.2$  and  $z = 0.2$ . We observe that IPM performs its best with  $z = 0.4$ ; hence, in our results, we report the performance with  $z = 0.4$ . For the optimized attacks, we use aggregator agnostic Min-sum and Min-max attacks [39] using the  $\sigma_t$  as the initial perturbation vector.

4) *Hybrid Sparse Attacks*:: In our experiments, we consider four different variations of our sparse Byzantine attack framework. First, we consider base strategy  $\Pi_r(\delta)$  that generates a sparse mask with a sparsity ratio of  $\delta$ , randomly without any constraint; for the second strategy, we impose

a constraint that the sparsity ratio of  $\delta$  is achieved at each layer, which is denoted by  $\Pi_{lr}(\delta)$ . Finally, for the last two strategies, we modify the first two strategies by inducing the constraint that the critical layers should be non-sparse, i.e.,  $\delta_l = 1$ , for  $l \in \mathcal{L}_{critical}$ , which are denoted with  $\Pi_{lr}^+(\delta)$  and  $\Pi_{lr}^+(\delta)$ , respectively. In addition to random sparsity, we also consider ERK [13] method to obtain sparsity patterns for each individual layer, denoted by  $\Pi_{ERK}^+(\delta)$ , and finally, utilize the network pruning-based attack, using FORCE algorithm, which is denoted by  $\Pi_{FC}^+(\delta)$ .

## B. Experimental Results

To analyze the effectiveness of our proposed solution, we have performed extensive simulations by measuring its impact on existing SoTA robust aggregators, namely, TM [52], CC [24], Bulyan [12], Multi-Krum [6], RFA [36], SignSGD (Majority Voting) [3] and two different implementations (utilize Krum or Bulyan) of recent SoTA defence mechanism GAS [30]. For the fair performance comparison, we consider the existing attacks under two categories based on whether they are dynamically optimized at each round or utilize a fixed policy. In the first category, the attacks with fixed policy, we consider bit-flip, label-flip, ALIE [2], IPM [48] and ROP [54]. In the second category, we consider dynamically optimized attacks Min-Sum [39] and Min-Max [39].

In Table VI, we demonstrate the final test accuracy results for CIFAR-10 dataset with IID-distribution and ResNet-20 architecture. For the sake of presentation, we highlight the best Attack performance for those who utilize fixed policy in addition to individual performances. For our proposed Hybrid sparse attack we consider all four variations of the random sparsity masks under four different sparsity regime, i.e.,  $\delta = \{5 \times 10^{-3}, 5 \times 10^{-2}, 2 \times 10^{-1}, 5 \times 10^{-1}\}$  as well as the mask generated by FORCE for  $\delta = 5 \times 10^{-3}$ . The corresponding test accuracy results are illustrated in Table VI. One of our immediate observations is that both variations of the GAS defence mechanism are highly effective against fixed policy attacks; we observe minimum test accuracy of %85 except for our proposed hybrid sparse attack. Regarding the performance of the proposed hybrid sparse attack, we observe that, in the case of randomly generated sparsity mask, the best performance is obtained with  $\Pi_{lr}^+(\delta)$  which induces a layer-wise sparsity constraint and identifies the critical layers and often it performs best for moderate sparsity regime  $\delta = 2 \times 10^{-1}$  and the strength of the hybrid sparse attack weakens with decreasing the sparsity ratio. Also the performance comparison of  $\Pi_{lr}(\delta)$  and  $\Pi_{lr}^+(\delta)$  clearly highlights the importance of targeting critical layers.

To test the advantage of the side information regarding synaptic connectivity on the performance of the attack, we compare the performance of the attack generated according to  $\Pi_{lr}^+(\delta)$  and the one generated according to pruning strategy  $\Pi_{FC}^+(\delta)$ , under the same sparsity constraint  $\delta = 5 \times 10^{-3}$ . Contrary to our initial argument that attacking specific locations that exhibit certain vital connectivity patterns enhances the strength of the attack, on average, we do not observe a

visible improvement in the impact of the hybrid sparse attack. However, the interesting observation is that in the case of CC, which re-scales the adversarial perturbation without changing the direction, the mask obtained through pruning provides a significant observation, as illustrated in Table VI. At this point, we recall that NN pruning strategies often overemphasize certain layers; hence, while taking the topology-based connectivity and sensitivity patterns into account for targeting enhances the impact of attack, which is visible in the case of CC, accumulation of attack at certain layers may make attack to relinquish its imperceptibility.

To verify the argument above, we follow a strategy where we again utilize the FORCE algorithm to perform network pruning but induce an additional constraint on the FC layer, i.e.,  $\delta_{FC}^{max} = 2 \times 10^{-1}$ , in order to achieve a sparsity mask where non-sparse positions are distributed more uniformly compared to the previous case, where most of them accumulated at FC layer. The results back our argument, and visible improvements are observed in the performance, especially against the GAS defence mechanism, which divides the vector into smaller sub-vectors and performs aggregation for each sub-vector separately. For the completeness of our analysis regarding the relation between the sparsity pattern and the attack performance, we further utilize the ERK-base sparsity masks [13], which divides the sparsity budget among the layers according to the number of incoming and outgoing connections between the hidden layers. [Rewrite] However, similar to the FORCE, which overemphasizes the initial conv layer and particularly the penultimate FC layer, the ERK method overemphasizes the initial conv layer, where all the weights are preserved as illustrated in 1 with the green colour. Hence, similar to vanilla FORCE, the overemphasized initial conv layer makes the ERK method less desirable against certain defence mechanisms, especially on GAS. Overall, from the discussion above, we conclude that there is a certain trade-off regarding the formation of the attack; the underlying sparsity mask should be designed in parallel to the topology-based connectivity and sensitivity patterns identified through network pruning, but also the position of the non-sparse weights, where the attack targets more aggressively, should be not be concentrated at particular layers. As we already discuss above, such unintended concentration can be mitigated by enforcing a layer-wise sparsity constraint. Through extensive simulations, we have analyzed various alternatives for regularizing the layer-wise sparsity, and the best yet simple solution is to have a constraint for the FC layer with  $\delta_{FC}^{max}$ . Next, we repeat the same simulation for the non-iid data distribution scenario, and the results are illustrated in Table VII. In this more practical scenario, we have shown that the proposed hybrid sparse attack surpasses all the known defence mechanisms, including GAS, which is effective against all fixed policy Byzantine attacks, almost achieves Byzantine-free accuracy, and makes a model diverge. One of the key aspects here is that the performance of  $\Pi_{FC}^+(\delta)$ , compared to its baseline form ALIE, demonstrates how attacking only a very limited number of carefully selected weights enhances the strength of

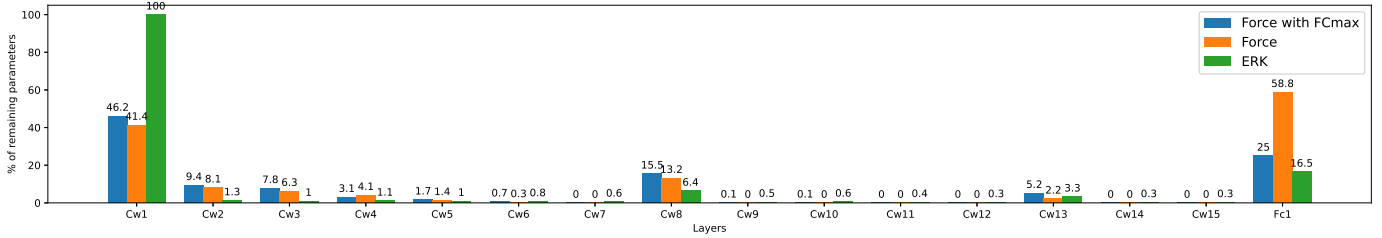


Fig. 1: Distribution of the non-sparse locations (remaining weights) in ResNet-20 architecture after pruning with ERK, Vanilla Force and Force with sparsity constraint on FC layer,  $\delta_{FC}^{max} = 0.25$ , for  $\delta = 0.005$ . The x-axis denotes the NN layers, where  $Cw_i$  denotes the weights of the  $i$ th convolutional layer, and Fc1 denotes the weights of the fully connected layer at the end.

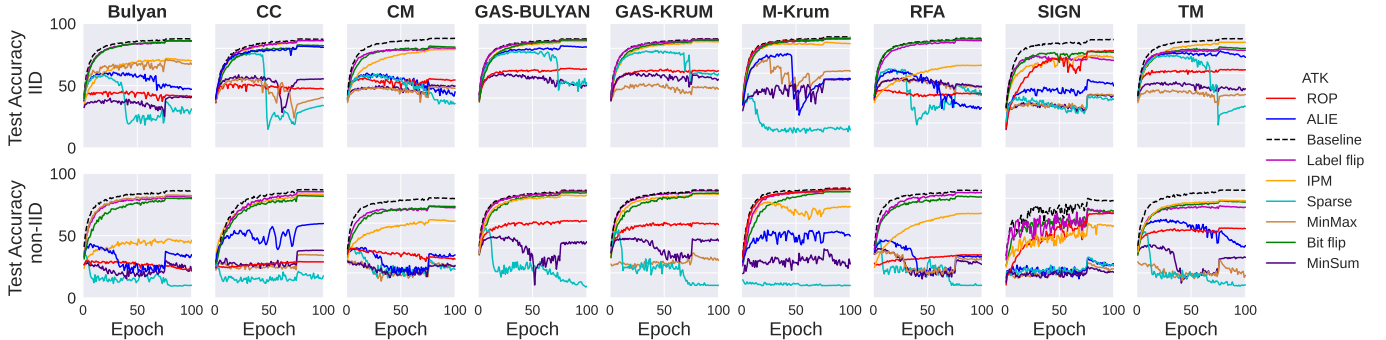


Fig. 2: Test accuracy results of training ResNet-20 architecture with Cifar-10 dataset distributed IID and non-IID over  $k = 25$  client  $k_m = 5$  of them being malicious. The training and testing are performed over 100 epochs and repeated for 9 different aggregation mechanisms and under 8 different Byzantine attack strategies. The reported results are obtained by averaging 3 number of independent trials.

the attack significantly. Consequently, the simulation results obtained for ALIE, Min-Sum, and hybrid sparse attack, where all three strategies utilize the same base attack formation, demonstrate that the level of aggressiveness and the carefully chosen target locations significantly increase the strength of the attack, which particularly visible in the case of GAS defence.

Finally, to better illustrate the impact of various Byzantine strategies against the convergence of the training process orchestrated by different robust aggregators, we plot the convergence dynamics in Fig. 2, for the both IID and Non-IID scenarios.

## V. CONCLUSIONS

In this work, we introduce a novel Byzantine attack framework that has been designed to be effective against different types of defence mechanisms simultaneously. The proposed framework generates an attack by combining two components: sparse but more aggressive and dense but more stealthy, forming a stronger but imperceptible attack. Further, by utilizing a network pruning framework, we identify the sensitive locations, those later targeted by the sparse component of the Byzantine attack, to increase the strength of the attack. Finally, through extensive simulations over different NN networks, datasets and defence mechanisms, we have shown the effectiveness of our approach. Overall, in this work, we have

initiated the discussion of how the existing form of the Byzantines can be enhanced by exploring the nature of the network topology, and we believe our extensive analysis will draw further attention and possibly lead to a new research direction in the robust federated learning context. In the scope of this work, we have limited our focus to extracting certain topology based side information (identifying certain important/sensitive weights) to scale the base adversarial perturbation accordingly, as a future research direction, we are planning to design a framework where the direction of the perturbations is also determined with respect to the network topology.

TABLE VII: Final test accuracy results of training ResNet-20 architecture with Cifar-10 dataset distributed non-IID over  $k = 25$  client  $k_m = 5$  of them being malicious. The training is performed over 100 epochs and repeated for 8 different aggregation mechanisms and under 8 different Byzantine attack strategies. The reported results are obtained by averaging 3 number of independent trials. We use **blue**, **red** and **green** to highlight the best results for fixed policy attacks, ALIE, Bit Flip, IPM, Label Flip, ROP dynamically optimized attacks, Min-Sum, Min-Max and proposed sparse hybrid attack variations with different sparsity constraint  $\delta$ , respectively, and we underline the best attack result against each defence mechanism.

Method / AGGR	Bulyan	CC	CM	M-Krum	RFA	TM	GAS-KRUM	GAS-Bulyan
<b>No ATK</b>	86.04 ± 0.47	86.87 ± 0.3	79.94 ± 0.43	88.1 ± 0.4	86.44 ± 0.72	86.66 ± 0.53	86.66 ± 0.49	86.31 ± 0.49
ALIE	34.73 ± 0.69	59.72 ± 3.42	34.48 ± 1.89	<b>49.66 ± 9.25</b>	<b>32.85 ± 3.35</b>	<b>42.07 ± 7.2</b>	<b>57.0 ± 11.37</b>	63.62 ± 5.28
Bit Flip	79.76 ± 1.04	81.79 ± 0.49	73.54 ± 1.15	85.25 ± 0.52	80.94 ± 0.64	76.99 ± 1.29	84.22 ± 0.31	84.48 ± 0.24
IPM	46.26 ± 0.88	83.26 ± 0.7	61.87 ± 4.58	73.18 ± 3.9	67.88 ± 1.91	77.88 ± 1.9	83.31 ± 0.61	82.35 ± 0.74
Label Flip	80.88 ± 1.03	85.23 ± 0.39	72.44 ± 0.24	87.31 ± 0.32	84.63 ± 0.03	72.95 ± 1.5	85.95 ± 0.55	85.55 ± 0.34
ROP	<b>22.46 ± 5.42</b>	<b>28.93 ± 1.11</b>	<b>31.19 ± 2.41</b>	87.3 ± 0.73	34.39 ± 1.99	55.6 ± 1.59	64.63 ± 1.74	<b>62.52 ± 1.19</b>
<b>Best Attack *</b>	22.46 ± 5.42	28.93 ± 1.11	31.19 ± 2.41	49.66 ± 9.25	34.39 ± 1.99	42.07 ± 7.2	57.0 ± 11.37	62.52 ± 1.19
Min-Sum	<b>21.59 ± 4.12</b>	38.08 ± 2.63	26.08 ± 2.48	<b>27.19 ± 5.87</b>	<b>26.83 ± 2.2</b>	32.48 ± 1.94	45.77 ± 4.67	<b>45.15 ± 5.78</b>
Min-Max	82.21 ± 0.12	<b>34.04 ± 1.4</b>	<b>25.98 ± 2.98</b>	86.89 ± 0.51	30.19 ± 2.21	<b>18.03 ± 1.54</b>	<b>30.05 ± 16.57</b>	85.89 ± 0.42
$\Pi_r(\delta = 5 \times 10^{-3})$	22.74 ± 2.4	47.4 ± 2.25	26.96 ± 1.7	27.37 ± 4.12	33.84 ± 10.12	36.56 ± 7.23	59.96 ± 4.97	48.11 ± 13.35
$\Pi_r(\delta = 5 \times 10^{-2})$	18.95 ± 2.18	25.22 ± 3.37	28.13 ± 1.66	13.57 ± 3.53	28.27 ± 5.97	37.8 ± 8.69	59.37 ± 3.24	43.02 ± 7.57
$\Pi_r(\delta = 2 \times 10^{-1})$	11.71 ± 1.43	19.57 ± 2.39	27.3 ± 1.09	10.04 ± 0.06	39.79 ± 6.29	23.92 ± 8.62	55.63 ± 8.78	23.36 ± 7.91
$\Pi_r(\delta = 5 \times 10^{-1})$	25.48 ± 4.24	<b>15.41 ± 3.46</b>	20.88 ± 2.88	9.9 ± 0.56	28.87 ± 8.89	<b>10.0 ± 0.0</b>	57.33 ± 4.99	53.34 ± 8.65
$\Pi_r^+(\delta = 5 \times 10^{-3})$	9.73 ± 0.59	20.09 ± 1.61	22.51 ± 4.25	11.86 ± 1.59	11.3 ± 1.84	33.97 ± 7.44	36.48 ± 10.87	31.07 ± 6.62
$\Pi_r^+(\delta = 5 \times 10^{-2})$	12.18 ± 2.22	17.34 ± 4.88	22.14 ± 1.37	11.96 ± 2.52	10.0 ± 0.0	25.69 ± 7.31	33.21 ± 13.93	10.0 ± 0.0
$\Pi_r^+(\delta = 2 \times 10^{-1})$	17.96 ± 6.48	18.27 ± 1.32	27.27 ± 1.03	11.09 ± 1.57	10.0 ± 0.0	10.01 ± 0.01	41.3 ± 6.21	15.61 ± 8.46
$\Pi_r^+(\delta = 5 \times 10^{-1})$	16.42 ± 2.35	16.57 ± 3.2	23.25 ± 1.08	9.71 ± 0.27	14.51 ± 3.32	<b>10.0 ± 0.0</b>	19.18 ± 3.44	60.35 ± 5.04
$\Pi_{lr}(\delta = 5 \times 10^{-3})$	24.06 ± 1.46	56.06 ± 1.81	32.75 ± 2.96	45.4 ± 5.98	28.89 ± 7.26	46.65 ± 1.43	45.33 ± 3.25	43.87 ± 11.0
$\Pi_{lr}(\delta = 5 \times 10^{-2})$	22.84 ± 4.02	25.7 ± 4.03	25.95 ± 5.18	9.41 ± 1.53	44.18 ± 7.48	43.24 ± 8.61	61.14 ± 4.62	57.16 ± 6.89
$\Pi_{lr}(\delta = 2 \times 10^{-1})$	16.96 ± 6.18	20.73 ± 2.51	27.63 ± 0.73	22.02 ± 7.64	27.98 ± 8.25	32.66 ± 1.65	51.07 ± 12.81	38.03 ± 5.0
$\Pi_{lr}(\delta = 5 \times 10^{-1})$	19.39 ± 4.05	15.85 ± 2.0	20.98 ± 4.08	10.78 ± 1.18	25.24 ± 2.47	<b>10.0 ± 0.0</b>	54.67 ± 4.5	48.17 ± 11.51
$\Pi_{lr}^+(\delta = 5 \times 10^{-3})$	10.11 ± 0.03	25.11 ± 1.05	27.99 ± 2.51	14.02 ± 2.14	10.0 ± 0.0	23.3 ± 4.98	34.71 ± 3.65	21.67 ± 4.19
$\Pi_{lr}^+(\delta = 5 \times 10^{-2})$	10.31 ± 1.27	16.68 ± 3.68	23.33 ± 3.51	10.3 ± 0.41	10.0 ± 0.0	27.39 ± 9.94	22.2 ± 8.98	11.29 ± 1.82
$\Pi_{lr}^+(\delta = 2 \times 10^{-1})$	12.63 ± 1.71	18.8 ± 0.44	24.73 ± 2.48	10.25 ± 0.35	12.08 ± 2.93	11.68 ± 1.2	34.92 ± 16.93	22.29 ± 13.13
$\Pi_{lr}^+(\delta = 5 \times 10^{-1})$	22.23 ± 4.22	17.79 ± 3.21	21.73 ± 1.41	9.7 ± 0.23	29.02 ± 7.81	<b>10.0 ± 0.0</b>	11.8 ± 2.36	51.62 ± 10.66
$\Pi_{ERK}^+(\delta = 5 \times 10^{-3})$	15.49 ± 5.99	15.82 ± 3.36	22.13 ± 1.38	10.03 ± 0.7	<b>9.41 ± 0.83</b>	10.0 ± 0.0	10.0 ± 0.0	10.0 ± 0.0
$\Pi_{ERK}^+(\delta = 5 \times 10^{-2})$	64.01 ± 8.4	61.59 ± 2.58	27.93 ± 3.56	48.92 ± 8.47	54.25 ± 4.71	41.33 ± 3.68	47.92 ± 10.8	71.43 ± 4.58
$\Pi_{ERK}^+(\delta = 2 \times 10^{-1})$	70.02 ± 3.23	52.71 ± 4.45	27.81 ± 2.11	46.76 ± 9.56	49.88 ± 4.37	26.18 ± 2.8	32.47 ± 2.22	71.08 ± 2.33
$\Pi_{ERK}^+(\delta = 5 \times 10^{-1})$	78.71 ± 3.46	41.61 ± 1.3	23.24 ± 2.41	47.92 ± 2.2	26.6 ± 6.46	20.67 ± 1.52	22.34 ± 3.55	72.27 ± 19.0
$\Pi_F^+(\delta = 5 \times 10^{-3})$	26.31 ± 3.41	24.28 ± 2.96	26.41 ± 2.33	10.93 ± 1.31	39.57 ± 5.77	10.0 ± 0.0	<b>10.0 ± 0.0</b>	64.26 ± 7.74
$\Pi_F^+(\delta = 5 \times 10^{-3})$ ( $\delta_{FC}^{max} = 0.25$ )	<b>9.93 ± 0.3</b>	17.61 ± 4.04	22.89 ± 2.13	9.84 ± 0.14	10.0 ± 0.0	<b>10.0 ± 0.0</b>	10.01 ± 0.01	<b>9.24 ± 1.08</b>
$\Pi_F^+(\delta = 1 \times 10^{-2})$ ( $\delta_{FC}^{max} = 0.25$ )	10.29 ± 0.42	16.23 ± 3.5	<b>19.89 ± 1.54</b>	<b>8.79 ± 2.3</b>	10.0 ± 0.0	<b>10.0 ± 0.0</b>	<b>10.0 ± 0.0</b>	10.0 ± 0.0

## REFERENCES

- [1] E. Bagdasaryan, A. Veit, Y. Hua, D. Estrin, and V. Shmatikov, “How to backdoor federated learning,” in *AISTATS*, 2020.
- [2] G. Baruch, M. Baruch, and Y. Goldberg, “A little is enough: Circumventing defenses for distributed learning,” in *NeurIPS*, 2019.
- [3] J. Bernstein, J. Zhao, K. Aizzadenesheli, and A. Anandkumar, “sgnsgd with majority vote is communication efficient and fault tolerant,” in *ICLR*, 2019.
- [4] A. N. Bhagoji, S. Chakraborty, P. Mittal, and S. Calo, “Analyzing federated learning through an adversarial lens,” in *ICML*, 2019.
- [5] B. Biggio, B. Nelson, and P. Laskov, “Poisoning attacks against support vector machines,” in *ICML*, 2012.
- [6] P. Blanchard, E. M. El Mhamdi, R. Guerraoui, and J. Stainer, “Machine learning with adversaries: Byzantine tolerant gradient descent,” in *NIPS*, 2017.
- [7] X. Cao, M. Fang, J. Liu, and N. Z. Gong, “Fltrust: Byzantine-robust federated learning via trust bootstrapping,” *arXiv preprint arXiv:2012.13995*, 2020.
- [8] X. Chen, T. Chen, H. Sun, S. Z. Wu, and M. Hong, “Distributed training with heterogeneous data: Bridging median-and mean-based algorithms,” *Advances in Neural Information Processing Systems*, vol. 33, pp. 21 616–21 626, 2020.
- [9] P. de Jorge, A. Sanyal, H. Behl, P. Torr, G. Rogez, and P. K. Dokania, “Progressive skeletonization: Trimming more fat from a network at initialization,” in *International Conference on Learning Representations*, 2021.
- [10] E.-M. El-Mhamdi, R. Guerraoui, A. Guirguis, L. N. Hoang, and S. Rouault, “Genuinely distributed byzantine machine learning,” ser. PODC ’20. New York, NY, USA: Association for Computing Machinery, 2020, p. 355–364. [Online]. Available: <https://doi.org/10.1145/3382734.3405695>
- [11] E.-M. El-Mhamdi, R. Guerraoui, and S. Rouault, “Distributed momentum for byzantine-resilient stochastic gradient descent,” in *ICLR*, 2021.
- [12] E. M. El Mhamdi, R. Guerraoui, and S. Rouault, “The hidden vulnerability of distributed learning in byzantium,” in *ICML*, 2018.
- [13] U. Evcı, T. Gale, J. Menick, P. S. Castro, and E. Elsen, “Rigging the lottery: Making all tickets winners,” in *Proceedings of the 37th International Conference on Machine Learning*, 2020.
- [14] M. Fang, X. Cao, J. Jia, and N. Z. Gong, “Local model poisoning attacks to byzantine-robust federated learning,” in *USENIX Conference on Security Symposium*, 2020.
- [15] S. Farhadkhani, R. Guerraoui, N. Gupta, R. Pinot, and J. Stephan, “Byzantine machine learning made easy by resilient averaging of momentums,” in *International Conference on Machine Learning*. PMLR, 2022, pp. 6246–6283.
- [16] J. Frankle and M. Carbin, “The lottery ticket hypothesis: Finding sparse, trainable neural networks,” in *International Conference on Learning Representations*, 2019. [Online]. Available: <https://openreview.net/forum?id=rJl-b3RcF7>
- [17] C. Fung, C. J. Yoon, and I. Beschastnikh, “The limitations of federated learning in sybil settings,” in *Usenix RAID*, 2020.
- [18] E. Gorbunov, S. Horváth, P. Richtárik, and G. Gidel, “Variance reduction is an antidote to byzantines: Better rates, weaker assumptions and communication compression as a cherry on the top,” 2022.
- [19] R. Guerraoui, N. Gupta, R. Pinot, S. Rouault, and J. Stephan, “Differential privacy and byzantine resilience in sgd: Do they add up?” ser. PODC’21. New York, NY, USA: Association for Computing Machinery, 2021, p. 391–401. [Online]. Available: <https://doi.org/10.1145/3465084.3467919>
- [20] A. Gupta, T. Luo, M. V. Ngo, and S. K. Das, “Long-short history of gradients is all you need: Detecting malicious and unreliable clients in federated learning.” Berlin,

- Heidelberg: Springer-Verlag, 2022, p. 445–465. [Online]. Available: [https://doi.org/10.1007/978-3-031-17143-7\\_22](https://doi.org/10.1007/978-3-031-17143-7_22)
- [21] N. Gupta and N. H. Vaidya, “Fault-tolerance in distributed optimization: The case of redundancy,” in *Proceedings of the 39th Symposium on Principles of Distributed Computing*, ser. PODC ’20. New York, NY, USA: Association for Computing Machinery, 2020, p. 365–374. [Online]. Available: <https://doi.org/10.1145/3382734.3405748>
  - [22] K. He, X. Zhang, S. Ren, and J. Sun, “Deep residual learning for image recognition,” in *Proceedings of the IEEE conference on computer vision and pattern recognition*, 2016.
  - [23] R. Jin, Y. Huang, X. He, H. Dai, and T. Wu, “Stochastic-sign sgd for federated learning with theoretical guarantees,” *arXiv preprint arXiv:2002.10940*, 2020.
  - [24] S. P. Karimireddy, L. He, and M. Jaggi, “Learning from history for byzantine robust optimization,” in *ICML*, 2021.
  - [25] —, “Byzantine-robust learning on heterogeneous datasets via bucketing,” in *ICLR*, 2022.
  - [26] J. Konečný, H. B. McMahan, F. X. Yu, P. Richtárik, A. T. Suresh, and D. Bacon, “Federated learning: Strategies for improving communication efficiency,” *NIPS workshop on Private Multiparty Machine Learning*, 2016.
  - [27] A. Krizhevsky, V. Nair, and G. Hinton, “Cifar-10 (canadian institute for advanced research).”
  - [28] Y. LeCun and C. Cortes, “MNIST handwritten digit database,” 2010. [Online]. Available: <http://yann.lecun.com/exdb/mnist/>
  - [29] N. Lee, T. Ajanthan, and P. Torr, “SNIP: SINGLE-SHOT NETWORK PRUNING BASED ON CONNECTION SENSITIVITY,” in *International Conference on Learning Representations*, 2019. [Online]. Available: <https://openreview.net/forum?id=B1VZqjAcYX>
  - [30] Y. Liu, C. Chen, L. Lyu, F. Wu, S. Wu, and G. Chen, “Byzantine-robust learning on heterogeneous data via gradient splitting,” in *Proceedings of the 40th International Conference on Machine Learning*, ser. ICML’23. JMLR.org, 2023.
  - [31] B. McMahan, E. Moore, D. Ramage, S. Hampson, and B. A. y Arcas, “Communication-efficient learning of deep networks from decentralized data,” in *AISTATS*, 2017.
  - [32] T. Minka, “Estimating a dirichlet distribution,” 2000.
  - [33] L. Muñoz-González, K. T. Co, and E. C. Lupu, “Byzantine-robust federated machine learning through adaptive model averaging,” *arXiv preprint arXiv:1909.05125*, 2019.
  - [34] J. Peng, W. Li, and Q. Ling, “Variance reduction-boosted byzantine robustness in decentralized stochastic optimization,” in *ICASSP 2022 - 2022 IEEE International Conference on Acoustics, Speech and Signal Processing (ICASSP)*, 2022, pp. 4283–4287.
  - [35] J. Peng, Z. Wu, and Q. Ling, “Byzantine-robust variance-reduced federated learning over distributed non-i.i.d. data,” *CoRR*, vol. abs/2009.08161, 2020. [Online]. Available: <https://arxiv.org/abs/2009.08161>
  - [36] K. Pillutla, S. M. Kakade, and Z. Harchaoui, “Robust aggregation for federated learning,” *IEEE Transactions on Signal Processing*, 2022.
  - [37] M. Raynal, D. Pasquini, and C. Troncoso, “Can decentralized learning be more robust than federated learning?” *arXiv preprint arXiv:2303.03829*, 2023.
  - [38] M. Raynal and C. Troncoso, “On the conflict of robustness and learning in collaborative machine learning,” *arXiv preprint arXiv:2402.13700*, 2024.
  - [39] V. Shejwalkar and A. Houmansadr, “Manipulating the byzantine: Optimizing model poisoning attacks and defenses for federated learning,” in *NDSS*, 2021.
  - [40] V. Shejwalkar, A. Houmansadr, P. Kairouz, and D. Ramage, “Back to the drawing board: A critical evaluation of poisoning attacks on production federated learning,” in *IEEE Symposium on Security and Privacy*, 2022.
  - [41] Z. Sun, P. Kairouz, A. T. Suresh, and H. B. McMahan, “Can you really backdoor federated learning?” *arXiv preprint arXiv:1911.07963*, 2019.
  - [42] H. Tanaka, D. Kunin, D. L. Yamins, and S. Ganguli, “Pruning neural networks without any data by iteratively conserving synaptic flow,” in *Advances in Neural Information Processing Systems*, H. Larochelle, M. Ranzato, R. Hadsell, M. Balcan, and H. Lin, Eds., vol. 33. Curran Associates, Inc., 2020, pp. 6377–6389.
  - [43] K. Varma, Y. Zhou, N. Baracaldo, and A. Anwar, “Legato: A layerwise gradient aggregation algorithm for mitigating byzantine attacks in federated learning,” in *2021 IEEE 14th international conference on cloud computing (CLOUD)*. IEEE, 2021, pp. 272–277.
  - [44] C. P. Wan and Q. Chen, “Robust federated learning with attack-adaptive aggregation,” *arXiv preprint arXiv:2102.05257*, 2021.
  - [45] Z. Wu, Q. Ling, T. Chen, and G. B. Giannakis, “Federated variance-reduced stochastic gradient descent with robustness to byzantine attacks,” *IEEE Transactions on Signal Processing*, vol. 68, pp. 4583–4596, 2020.
  - [46] H. Xiao, K. Rasul, and R. Vollgraf, “Fashion-mnist: a novel image dataset for benchmarking machine learning algorithms,” *ArXiv*, 2017.
  - [47] C. Xie, K. Huang, P.-Y. Chen, and B. Li, “Dba: Distributed backdoor attacks against federated learning,” in *ICLR*, 2020.
  - [48] C. Xie, O. Koyejo, and I. Gupta, “Fall of empires: Breaking byzantine-tolerant sgd by inner product manipulation,” in *Uncertainty in Artificial Intelligence*, 2020.
  - [49] C. Xie, S. Koyejo, and I. Gupta, “Zeno: Distributed stochastic gradient descent with suspicion-based fault-tolerance,” in *International Conference on Machine Learning*. PMLR, 2019, pp. 6893–6901.
  - [50] W. Xie, T. Pethick, A. Ramezani-Kebrya, and V. Cevher, “Mixed nash for robust federated learning,” *Transactions on Machine Learning Research*, 2023.
  - [51] C. Yin and Q. Zeng, “Defending against data poisoning attack in federated learning with non-iid data,” *IEEE Transactions on Computational Social Systems*, pp. 1–13, 2023.
  - [52] D. Yin, Y. Chen, R. Kannan, and P. Bartlett, “Byzantine-robust distributed learning: Towards optimal statistical rates,” in *ICML*, 2018.
  - [53] H. Zhu and Q. Ling, “Byzantine-robust aggregation with gradient difference compression and stochastic variance reduction for federated learning,” in *ICASSP 2022 - 2022 IEEE International Conference on Acoustics, Speech and Signal Processing (ICASSP)*, 2022, pp. 4278–4282.
  - [54] K. Özfatura, E. Özfatura, A. Küpçü, and D. Gunduz, “Byzantines can also learn from history: Fall of centered clipping in federated learning,” *IEEE Transactions on Information Forensics and Security*, vol. 19, pp. 2010–2022, 2024.

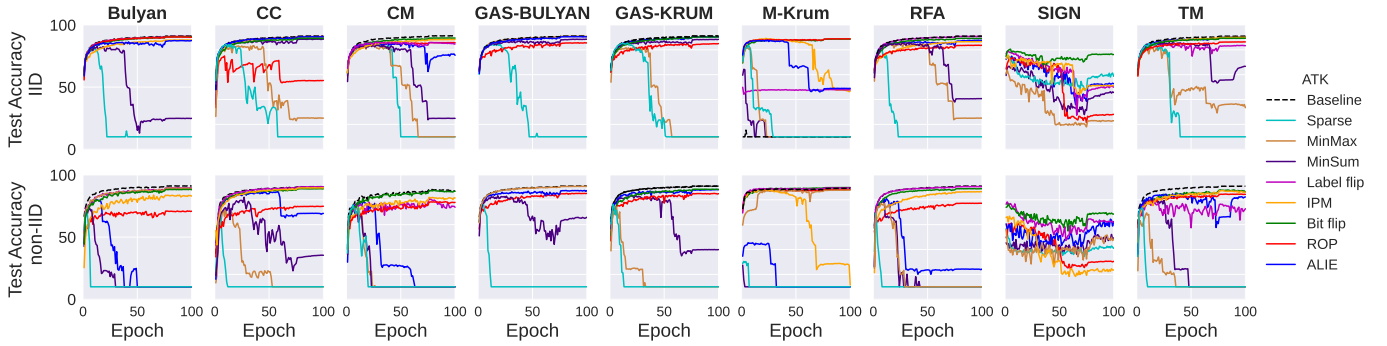


Fig. 3: Test accuracy results of training 2-Layer CNN architecture with FMNIST dataset distributed IID and non-IID over  $k = 25$  client  $k_m = 5$  of them being malicious. The training and testing are performed over 100 epochs and repeated for 9 different aggregation mechanisms and under 8 different Byzantine attack strategies. The reported results are obtained by averaging 3 number of independent trials.

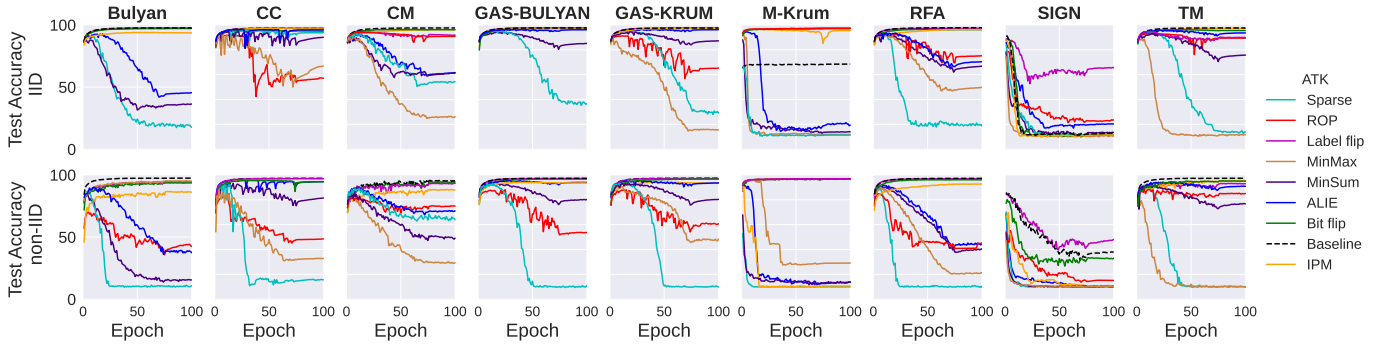


Fig. 4: Test accuracy results of training 2-Layer MLP architecture with MNIST dataset distributed IID and non-IID over  $k = 25$  client  $k_m = 5$  of them being malicious. The training and testing are performed over 100 epochs and repeated for 9 different aggregation mechanisms and under 8 different Byzantine attack strategies. The reported results are obtained by averaging 3 number of independent trials.

## APPENDIX

### A. Additional Numerical Results

Since smaller NN architectures are more vulnerable to Byzantine attacks, we mainly focus on moderately large NN architectures, i.e., ResNet-20, and the classification task on CIFAR-10. For the sake of completeness, in this subsection, we further conduct the same experiments with different NN networks and datasets, to be more precise, we have analyzed the byzantine performance and compare the existing attack and defence frameworks for the classification task on the FMNIST dataset with a 2-layer CNN architecture and classification task on MNIST dataset with 2-layer MLP architecture. For our hybrid sparse attack, we consider the configuration of  $\Pi_F^+(\delta = 5 \times 10^{-3}, \delta_{FC}^{max} = 0.25$  which often provides the best results in the case of CIFAR-10 dataset except the MNIST where we do not induce any limitation since MLP network only consist of fully connected layers as such we utilize  $\Pi_F^+(\delta = 1 \times 10^{-2}, \delta^{max}$  for MNIST classification task. The experimental results and the convergence behaviour under different robust aggregators and Byzantine attacks are illustrated in Fig. 3 and Fig. 4, respectively.

### B. Network Pruning

In this section, we further provide the details regarding the implementation of the FORCE network pruning framework.

1) *Sparsity Scheduler*: Similar to [9], we consider exponential decay sparsity scheduling that is over  $T$  pruning steps the number of non-sparse positions decreased from  $\kappa_0 = d$  to  $\kappa_T = \kappa$  gradually in the following manner:

$$\kappa_t = \lfloor e^{(\frac{t}{T} \log \kappa + (1 - \frac{t}{T}) \log d)} \rfloor.$$

2) *Pruning Algorithm*: The overall iterative pruning algorithm, executed over  $T$  steps with respect to the sparsity scheduling in eqn (B1), is illustrated in Algorithm 4, where at each iteration  $t$ , each byzantine node first computes the saliency  $\mathbf{s}_i(\boldsymbol{\theta}, \mathbf{c}_{t-1})$ , with respect to initial network weights  $\boldsymbol{\theta}$  and the precious binary sparsity mask  $\mathbf{c}_{t-1}$  according to eqn. (B1), then seek a consensus on the saliency measure. Then based on the saliency score, the non-sparse locations for the given scheduled sparsity constraint  $\kappa_t$ , simply through a  $Top_k$  operation.

---

**Algorithm 4** Iterative Network Pruning

---

- 1: **Inputs:** Target sparsity  $\kappa$ , Initialized weights  $\boldsymbol{\theta} \in \mathbb{R}^d$ , Time steps  $T$ , Local dataset  $\{D_i\}_{i \in \mathcal{K}_m}$
  - 2: **Outputs:**  $\mathbf{c}$
  - 3: Initialize  $\mathbf{c}_0 \leftarrow \mathbf{1}_d$
  - 4: Scheduled Sparsity  $\{\kappa_1, \dots, \kappa_T\}$  acc. eqn. (B1)
  - 5: **for**  $t = 1, \dots, T$  **do**,
  - 6:     **for**  $i \in \mathcal{K}_m$  **do**
  - 7:         Sample mini-batch:  $\zeta \in D_i$
  - 8:         Compute Saliency:  $\mathbf{s}_i(\boldsymbol{\theta}, \mathbf{c}_{t-1}) = |\boldsymbol{\theta} \odot \nabla F(\mathbf{c}_{t-1} \odot \boldsymbol{\theta}; \zeta)|$
  - 9:     Consensus Saliency:  $\mathbf{s}(\boldsymbol{\theta}, \mathbf{c}_{t-1}) \leftarrow \frac{1}{k_m} \sum_{i \in \mathcal{K}_m} \mathbf{s}_i(\boldsymbol{\theta}, \mathbf{c}_{t-1})$
  - 10:     Indices with maxim saliency measure  $\mathcal{I} = \text{Top}_{\kappa_t}(\mathbf{s})$
  - 11:     Update binary mask:  $\mathbf{c}_t \leftarrow \mathbf{c} : \mathbf{c}[i] = 1, \text{ if } i \in \mathcal{I}$
-